SCIEPublish

Article

Wind Influence on the Electrical Energy Production of Solar Plants

Carlos Bernardo [1], Ricardo A. Marques Lameirinhas [1,2,*], Catarina P. Correia V. Bernardo [1,2] and João Paulo N. Torres [2,3]

[1] Instituto Superior Tecnico, Avenida Rovisco Pais, 1, 1049-001 Lisboa, Portugal; carlosbernardoclopes@tecnico.ulisboa.pt (C.B.); catarina.bernardo@tecnico.ulisboa.pt (C.P.C.V.B.)
[2] Instituto de Telecomunicações, Avenida Rovisco Pais, 1, Torre Norte-10, 1049-001 Lisboa, Portugal; joaoptorres@hotmail.com (J.P.N.T.)
[3] Academia Militar/CINAMIL, Rua Gomes Freire 203, 1169-203 Lisboa, Portugal
* Corresponding author. E-mail: ricardo.lameirinhas@tecnico.ulisboa.pt (R.A.M.L.)

Received: 25 November 2023; Accepted: 12 February 2024; Available online: 20 February 2024

ABSTRACT: Solar energy, as a clean source of energy, plays a relevant role in this much desired (r)evolution. When talking about photovoltaics, despite the multiple studies on parameters that affect the panels operation, concrete knowledge on this matter is still in an incipient stage and precise data remains dispersed, given the mutability of outer factors beyond technology-related properties, hence the difficulties associated with exploration. Wind is one of them. Wind loads can affect the temperature of photovoltaics, whose efficiency is reduced when higher temperatures are reached. The viability of wind as natural cooling mechanism for solar plants and its influence on their electrical energy production is studied in this research work. Some appropriate results were achieved: depending on the module temperature prediction model used and on the photovoltaic technology in question, solar panels are foreseen to be up to approximately 3% more productive for average wind speeds and up to almost 7% more productive for higher speeds. Taking into consideration that wind speed values were collected in the close vicinity of the modules, these results can be proven to be even higher. That being said, this article contributes with accurate insights about wind influence on electrical energy production of solar plants.

Keywords: Optoelectronics; Photovoltaics; Renewable energies; Solar energy; Wind influence

1. Introduction

1.1. Photovoltaic Technology Era

Throughout the last years, the urge to reduce the usage of fossil fuels has been arising substantially, putting the conventional energy sources under a lot of pressure. Herewith, the demand for renewable energies is constantly increasing as a consequence of their significance as an alternative to the aforementioned sources. The five major renewable energy resources are wind, hydro, geothermal, biomass and solar. With their never-ending stamp at human scale, they play an imperative role in the ecological footprint, continually giving rise to new projects, new initiatives and also political decisions all over the world, seeking a solid environmental sustainability for the years yet to come [1–4].

That being said, a much more fruitful use of the renewable resources is crucial for answering the needs of populations and modern societies. In such a way, an ever-developing work has to be carried out by the many renewable related industries in order to improve effectiveness and efficiency. Amongst all the renewables, the usage of solar energy, although its recognised potential, still represents a small portion of the circle graph – a situation expected to change in the upcoming years [1–8]. With emerging solar PV technologies that show higher efficiencies and less costs, the referred fact is promised to change. With this in mind, as it can be considered that photovoltaics is still in an incipient phase due to their limitations in what concerns efficiency, several researches are on course in order to improve the operation of solar cells, either by, e.g., changing the designs, the structures or the materials, hence amplifying the reliability, spread and range of PV systems [3,7].

https://doi.org/10.35534/ces.2024.10004

With this in mind, this paper is suggested with the aim of contributing to the growth of solar photovoltaic technology in the sense that a wider knowledge of how external factors affect efficiency and maintenance of solar plants empowers a general perspective of project sizing and forthcoming topics of interest.

Facing many issues to what efficiency is concerned, PV panels are known to have their operation affected by temperature – ambient temperature and module temperature. Accordingly, higher temperatures are known to reduce power output of PV modules, as it will be further explained. High temperatures also represent a problem regarding panels lifetime, since that overheating can lead to destructive effects, such as cell or glass cracking, melting of solder or degradation of the solar cells [3,4,8]. This being the case, several cooling systems have been studied over the years, in order to avoid the issues aforesaid, being that some of them actually achieved relevant results. A consequent factor of these systems is an increase of investment and maintenance costs – a question to get around. Therefore, wind, being a natural and free-of-cost resource, emerges as a possible alternative to them. Nowadays, wind is still neglected when predicting modules temperatures, since that the Standard Approach (SA) – standard method of prediction panels temperatures – does not take wind variables into consideration. This has been proven to be far-fetched and some efforts have been made to change this procedure. With the purpose of improving guidelines for solar photovoltaic practices, distinct researchers have been trying to elaborate panel temperature prediction models that take wind data into account, as it is further shown.

1.2. Solar Cells Equivalent Models

Considering what was previously stated, the work performed and exploited in this work aims to identify the variation of modules temperature according to each panel temperature prediction model, to analyse this variation for various PV technologies, to verify the impact of different wind speeds in the variation of modules temperature and to examine how variations of panels temperature impact the output power of each module. All these topics culminate in the study of the viability of wind as a natural cooling mechanism for solar plants. Solar cells operation depends mainly on the amount of incident light. It is usually measured by a coefficient known as irradiance (or flux density), *G*, that is a measure of power incident per unit area – its respective units are W/m^2. Being an external factor, it varies depending on several aspects, such as the latitude, season and time of day at a given location. Furthermore, it is affected by other atmospheric conditions like clouds, dust or even relative humidity. Solar cells are known to behave like a diode, whose current flow, I_D, is given by Equation (1).

$$I_D = I_S\left(e^{\frac{U_D}{n\,U_T}} - 1\right) \tag{1}$$

where I_S is the diode reverse saturation current, U_D is the voltage applied across the diode, n is the diode ideality factor and U_T is the thermal voltage, that is equivalent to kT/q, in which k is the Boltzmann constant, T is the temperature and q is the electronic charge. As a result, for an ideal case, the current flow in a cell, I_{cell}, is given by Equation (2), having in mind that I_{PV} is the current generated by light [1–6].

$$I_{cell} = I_{PV} - I_D \tag{2}$$

Substituting expression 1 in expression 2, the final equation for the current flow in a solar cell is [1–6]:

$$I_{cell} = I_{PV} - I_S\left(e^{\frac{U_D}{n\,U_T}} - 1\right) \tag{3}$$

By simple inspection of the previous equation, it can be told that there is a relation of dependency between the current flow, I_{cell}, and the voltage across the diode, U_D.

From a theoretical point of view, it is possible to calculate the value of the Maximum Power Point (MPP) from the I–V curve and P–V curve that characterise a solar cell. These curves represent the relation between current, I_{cell}, and power, P, with voltage, U_D, respectively. For the referred calculation, Equation (4) is needed, where $C0$ is a constant dependent on the temperature of the solar cell, $C1$ is the coefficient of temperature of I_{PV}, ΔT is the difference between the temperature of the cell and the room temperature and, finally, G_{ref} is the reference irradiance (1000 W/m^2) [1–6].

$$I_{PV} = \left(C0 + C1\frac{\Delta T}{G_{ref}}\right)\cdot G \tag{4}$$

The MPP is a point (I,V) that maximises the area underneath the I–V curve. Therefore, the power of a solar cell and the maximum of its function is required. Given that

$$P = U \cdot I = U_D \left(I_{PV} - I_S \left(e^{\frac{U_D}{n\,U_T}} - 1 \right) \right) \tag{5}$$

And knowing that $e^{\frac{U_D}{n\,U_T}} \gg 1$ it can be said that:

$$P \sim U_D \left(I_{PV} - I_S \left(e^{\frac{U_D}{n\,U_T}} \right) \right) \tag{6}$$

Then, by deriving the power in function of the voltage (Equation (7)), it is possible to calculate the MPP, since it is the point where the prior derivative is null.

$$\frac{\mathrm{d}P}{\mathrm{d}U_D} = 0 \Leftrightarrow I_{PV} - I_S \left(e^{\frac{U_D}{n\,U_T}} \right) \left(1 + \frac{U_D}{n\,U_T} \right) = 0 \tag{7}$$

The short circuit, I_{SC}, is the point of maximum current that a solar cell achieves – it corresponds to U_D = 0 –, whereas the open circuit voltage, V_{OC}, is the point of maximum voltage of a solar cell – it corresponds to I_{cell} = 0. This being said, two equations that contribute to the understanding of solar cells operation are the short-circuit current variation with irradiance, Equation (8), and the open-circuit voltage variation with the relation $\frac{I_{SC}}{I_S}$, Equation (9), where I_{SCref} is the reference short-circuit current [1,2].

$$I_{SC} = \frac{G}{G_{ref}} I_{SC_{ref}} \tag{8}$$

$$V_{OC} = nU_T \ln\left(\frac{I_{SC}}{I_S} + 1 \right) \tag{9}$$

For a constant temperature, when the irradiance increases, the currents increase considerably, which means that I_{SC} will be much higher. On the other, the open-circuit voltage has only a slight increase. This can be proved theoretically by inspection of Equations (8) and (9). For a constant irradiance, I_{SC} remains approximately constant with an increase of temperature, having an unnoticeable elevation. Differently, the respective V_{OC} value decreases greatly with an increase of temperature, which can be induced by examination of the equations mentioned above [4,5].

1.3. Related Work

A brief analysis of the chosen literature is shown in order to present relevant related studies to the work that is going to be shown thereafter. Several important research findings will serve as a foundation to the calculations carried out in the last phase of this research.

In 2003, Tamizhmani et al. [9], based on IEEE PAR 1479 "Recommended Practice for the Evaluation of Photovoltaic Module Energy Production", proposed a method to predict power/energy production as a function of ambient temperature, T_a, wind speed (W_{speed}), wind direction (W_{dir}), total irradiance and relative humidity. They first developed a model based on the 5 inputs already mentioned and then tested another one based on 3 inputs only: ambient temperature, wind speed and global irradiance. They evaluated the two models by using a Neural Network from MATLAB Toolbox and explained that the 3 input model is more reliable due to lower related errors, as the errors in the measurement accuracy of wind direction and humidity may have a stronger influence than the two parameters themselves on the coefficient values; this phenomenon can be verified by their simulations, where several factors where compared, reaching a final conclusion: there is a simple linear relationship between the module temperature and the ambient conditions that can be simulated empirically by Equation (10), where the respective units are °C for T_a, W/m^2 for irradiance and m/s for wind speed.

$$T_m = 0.943 \cdot T_a + 0.028 \cdot G - 1.528 \cdot W_{speed} + 4.3 \tag{10}$$

This equation was formulated with the objective of fitting to all the different technologies under study and it is here classified as the Tamizhmani model.

In 2011, Ruscheweyh et al. [12] approached the effect of wind loads on solar plants placed on rooftops. They stated that there are some parameters that influence wind loads, such as the angle of the module to the horizontal plane, the distance of the module rows to each other, the position of the module in the module field, the gaps between the module's respective gap to the ground, the supporting system and many others. One of their main concerns was a phenomenon called the leading edge vortex – when there is a wind flow directed towards the building corner. In their research, they simulated the effect of wind in a wind tunnel by generating a wind profile, testing their model with a boundary layer for a free field.

Between a lot of concepts-description and further simulations, they came to the conclusion that all the results had the same tendency once the modules at the rim of the module field present the maximum wind load. This last-mentioned is reduced gradually when moving towards the rear field, which shows a significantly reduced load, due to the wind shadow effect.

In 2013, Schwingshackl et al. [13] compared the accuracy of different models that include and do not include wind data to predict PV cell temperature, assuming that the temperature of the model is the same as the cells' [14], they studied the cooling effect of wind on PV cell temperature for different cell technologies installed at a PV test facility in Bolzano, Italy, taking into consideration the module temperature as a function of solar irradiance, ambient temperature and wind, as shown in the prediction models below.

Schwingshackl et al. [13] performed in situ measurements, using sensors installed at a weather station placed next to the PV plant for obtaining the meteorological parameters. The PV cells temperature was recorded at the back of the modules. In addition to these measurements, they also used wind data from the European Centre for Medium-Range Weather Forecasts (ECMWF). Regarding the cell temperature prediction, eight models were used. The ones introduced here are the models pertinent to the developed work. As a consequence of their importance, their names are displayed in bold. All of these models relate the cells (therefore, the module) temperature with the incoming irradiance and relevant meteorological parameters.

The first model is the aforementioned Standard Approach, as expression 11, that is also known as the NOCT formula, in which the cell temperature is defined as T_c.

$$T_c = T_{a,NOCT} + \frac{G}{G_{NOCT}}\left(T_{NOCT} - T_{a,NOCT}\right) \tag{11}$$

In expression 11, G is the in-plane irradiance, T_{NOCT} is the nominal operating cell temperature, a factor whose value depends on the PV technology. G_{NOCT} and $T_{a,NOCT}$ are parameterised values: 800 W/m^2 and 20 °C, respectively. Although the full description of Nominal Operation Cell Temperature (NOCT) can be found in [15], it is important to know that it considers a wind speed of 1 m/s. The SA was the reference model used by Schwingshackl et al. and it is the model that will be used later as a reference when performing comparisons.

The second and third models are advanced models proposed by Skoplaki et al. [16], here called Skoplaki 1 and Skoplaki 2, respectively. As follows, they take wind data into account and both of them rely on expression 12.

$$T_c = T_a + \frac{G}{G_{NOCT}}\left(T_{NOCT} - T_{a,NOCT}\right) \cdot \frac{h_{w,NOCT}}{h_w} \cdot \left[1 - \frac{\eta_{STC}}{\tau \cdot \alpha}\left(1 - \beta_{STC} T_{STC}\right)\right] \tag{12}$$

There, h_w is the wind convection coefficient, $h_{w,NOCT}$ the wind convection coefficient at NOCT conditions (where W_{speed} = 1 m/s), η_{STC} is the efficiency of the module at STC, τ is the transmittance and α is the absorbance – their product is assumed to be equal to 0.9 [17] –, β_{STC} is the temperature coefficient of maximum power of the module and T_{STC} is the temperature at STC conditions, 25 °C. What differs between the two last-mentioned models is the parameterization of $h_w(v)$. Skoplaki 1 uses the parameterization developed by Skoplaki et al., as demonstrated in expression 13 and Skoplaki 2 refers to the parameterization suggested by Armstrong et al. [18], given by expression 14.

$$h_w = 5.7 + 2.8 W_{speed} \tag{13}$$

$$h_w = 8.3 + 2.2 W_{speed} \tag{14}$$

The wind speed is the local wind speed measured close to the module.

The fourth model was developed by Koehl et al. [19] but makes use of an empirical model advanced by Faimann [20]. In this way, Koehl et al. specify the values of the U0 and U1 constants for different PV cell technologies, which are used in expression 15 – equation that describes the Koehl model.

In an attempt to suggest an evolved prediction model, Mattei et al. [21] proposed one that says the PV cell temperature follows expression 16, where UPV is the heat exchange coefficient for the face of the module.

$$T_c = T_a + G \cdot \left(U0 + U1 \cdot W_{speed}\right) \tag{15}$$

$$T_c = \frac{U_{PV} T_a + G \cdot \left(\tau \cdot \alpha - \eta_{STC}(1 - \beta_{STC} T_{STC})\right)}{U_{PV} + \beta_{STC} \eta_{STC} G} \tag{16}$$

Since they refer two possible parameterizations for this variable, this implies the existence of two models: Mattei 1, in expression 17 and Mattei 2, in 18, following the procedure described for the Skoplaki models.

$$U_{PV} = 26.6 + 2.3 W_{speed} \tag{17}$$

$$U_{PV} = 24.1 + 2.9 W_{speed} \tag{18}$$

Similar to expression 13 and 14, W_{speed} is the wind speed measured close to the module.

Finally, a model proposed by Kurtz et al. [22] that does not consider parameters associated with each PV technology. This being said, the Kurtz model is in expression 19 and it proposes a correlation between cell temperature, ambient temperature, irradiance and wind speed given by:

$$T_c = T_a + G \cdot e^{-3.473-0.0594W_{speed}} \quad (19)$$

Likewise, the previous models, this one includes the local wind speed as a variable.

After comparing all the data obtained, Schwingshackl et al. stated that for p-Si cells, models Mattei 1 and Mattei 2 are the most accurate. When it comes to CdTe, they report that the SA and Kurtz model achieve the best results, indicating that it happens "probably because those PV modules have a higher thermal inertia than the silicon PV technologies" [13]. Nevertheless, they make it clear that since all PV technologies have different characteristics thus different behaviours, when estimating the temperature of the modules (taking wind data into account), it would be fallacious to select a generalised approach.

In 2016, Amajama et al. [23] studied the impact of wind on the output of a photovoltaic panel (mono-crystalline cell type), experimentally. The results were analysed by computing the output current and the output voltage versus wind speed at nearly constant air temperature, air pressure, relative humidity, and solar illuminance/intensity. Along with that, the relation between wind speed and solar illumination/intensity was tested, maintaining also the aforesaid parameters nearly constant. That being said, they state that wind speed, having an effect on radio waves propagation, aids it if the wind is flowing in parallel to the signal, but acts in the adverse way if it is tangential or anti-parallel, impairing the propagation of the radio waves. Moreover, they pointed out the similarity between these waves and electromagnetic radiations, that share comparable properties.

With the formerly mentioned in mind and following the data analysis, they attained two advantageous (A, B) and two disadvantageous (C, D) situations, respecting the performance of the PV module in function of the wind: (A) when wind is towards the front of an observer (or panel) with the sun some distance away in front; (B) when wind is towards the back of the observer (or panel) and the sun is behind; (C) when wind's direction is towards the back of an observer (or panel) and the sun is some distance in front of the observer (or panel); (D) when the sun is some distance behind the observer (or panel) and the wind direction is towards the front of the observer (or panel).

To sum up, in this last study, it was evidenced that, under the same conditions, when the molecular particles of the wind are in phase with the direction of the solar photonic particles, solar illuminance/intensity is favoured, thus unfavoured when out of phase. Consequently, the same phenomenon occurs in relation to the output of a photovoltaic panel [23].

2. Methodologies

The methodologies used are explained throughout this section. They refer to by what means the thematic introduced before was developed. Between all the new era softwares and available information, a major concern relies on how to gather trusted sources and achieve tangible and authentic results by simulation methods and calculations. Accordingly, following the equations that represent the operation of solar cells, it is imperative to estimate how wind and its mutable characteristics affect them and how it is revealed on the overall performance of the system. With the previously mentioned in mind, the equations already explained serve as a foundation to all of the remaining work.

As this paper is focused on the effect of wind (velocity and shadowing) on energy generation of solar plants – by studying the changes in temperature of solar cells according to the technologies and designs used –, the temperature values of the different modules had to be known. Having said that, the tools that allowed the acquisition of those values were the cell temperature prediction models mentioned previously, whose names are displayed in bold – Standard Approach, Skoplaki 1, Skoplaki 2, Koehl, Mattei 1, Mattei 2, Kurtz and Tamizhmani. As pointed out before, the reference model is the Standard Approach. Although the NOCT formula implies a wind speed of 1m/s, it does not take accurate wind data into account – despite wind's known volatility – and, notwithstanding its flaws, it is an industry standard method for calculating cells' temperature. Therefore, it becomes mandatory to cement fundamental notions when forecasting the power variation due to wind loads by consequent cell temperature fluctuations in solar plants. With this, temperature and resultant power deviations between all the models suggested were analysed in order to understand how different PV technologies behave upon different prediction models and different wind speeds.

This work was applied to all the modules present in the geometry detailed afterwards so as to investigate the effect of wind shadowing between PV arrays.

In order to perform complex engineering computations, a model of each of the intended PV geometries had to be created by scratch. For this task, a Computer-Aided Design (CAD) software is needed and the chosen softwares were

FreeCAD and Fusion 360. The first one was used to create the solar PV geometries and the later mentioned ensured the design of the wind tunnels. When it comes to Computational Fluid Dynamics (CFD), which is "a science that, with the help of digital computers, produces quantitative predictions of fluid flow phenomena based on the conservation laws (conservation of mass, momentum, and energy) governing fluid motion" [24], the software that allowed its concretion was Autodesk CFD – a CFD simulation software that engineers can use to predict how liquids and gases will perform when applied to some CAD geometry.

Once acquired the wind speed values by means of CFD, Microsoft Excel was the designated software to compute the calculations of the temperature (and associated peak power variation) for every single module, according to each (1) model, (2) solar cell technology and (3) wind speed value.

As this investigation intends to propose a general perspective on how wind affects the performance of solar plants, it was required that the CFD simulations were based on suitable and concrete data, such as realistic atmospheric conditions and characteristic values, for instance, the parameters of solar cells, dimensions of the PV modules and the support system designs. In what wind speeds are concerned, as there are multiple sources of meteorological information, it was taken into account data made available by Instituto Portugues do Mar e da Atmosfera (IPMA) and Meteored. After analysing the maximum and average wind speed values for the Lisbon district throughout the year 2020, two final values were established: W_{avg} = 4.06 m/s – Average Average Wind Speed – and W_{max} = 17.55 m/s – Average Maximum Wind Speed. Since that all module temperature prediction models consider T_a and G – ambient temperature and irradiance, respectively – and that NOCT conditions require G_{NOCT} = 800 W/m^2 and $T_{a,NOCT}$ = 20 °C, the values chosen for the in-plane irradiance and ambient temperature are the same as the NOCT ones so that $G = G_{NOCT}$ = 800 W/m^2 and $T_a = T_{a,NOCT}$ = 20 °C.

Given that there are many PV cells technologies, it is imperative to simulate the most convenient ones. With this purpose, p-Si, CdTe and CIGS technologies were the ones selected. Being that different technologies behave differently due to their intrinsic characteristics and, as beforesaid, aiming to the most accurate real-life simulation results, three distinct solar panels datasheets were collected – one for each technology. These datasheets can be found in [25,26,27], respectively. Their main characteristics (that are fundamental for the calculations) are expressed in Table 1.

Table 1. Main parameters for each solar cell technology.

	Technology		
Parameter	p-Si	CdTe	CIGS
H (%)	15.6	17.0	13.9
β_{STC} (%/°C)	−0.39	−0.28	−0.31
T_{NOCT} (°C)	45	45	47
Koehl Coefficient U0	30.02	23.37	22.19
Koehl Coefficient U1	6.28	5.44	4.09

Before proceeding to the computational simulations, a CAD geometry of the PV arrays had to be created having in mind its real dimensions. Understanding that each company produces PV modules of distinct sizes, it would not be adequate to simulate different geometries and then compare the results obtained, given that the design of each structure influences the aerodynamics hence the wind speeds around solar panels, which would lead to misleading results. For this reason, only one geometry was considered, having in mind that the Temperature Coefficient of P_{mpp}, β_{STC}, and the remaining parameters accounted in every cell temperature prediction model are technology/material-specific and their value is not dictated by module's dimension. The dimensions used for constructing the CAD models were 1645 × 992 × 35 mm, that correspond to the p-Si panels. That being said, two geometries were created, as seen in Figures 1 and 2 – arrays of three and nine panels, respectively, in two parallel rows, distancing 2140 mm from each other.

For the purpose of studying wind flow around the panels, CFD simulations demand that the geometries created have to be inside a wind tunnel. Assuming h as the total height of the CAD model, w its total width and l its total length, tunnels were created respecting the following rules proposed by Autodesk, the company that developed Autodesk CFD [26]: 3h <th < 4h – model sitting on the floor (z = 0) and th being the tunnel height; 5w <tw < 7w – model in the center and being tw the tunnel width; tunnel length from the front (inlet) to the object equal to 2l (in the direction of flow); tunnel length from the object to the back (outlet) and equal to 4l (in the direction of flow).

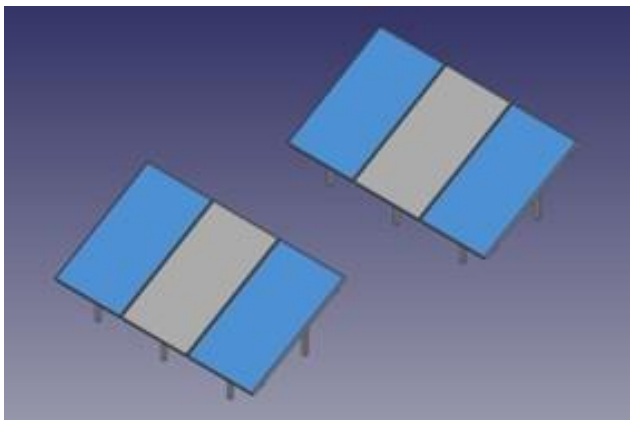

Figure 1. Two rows of arrays (3 by 2).

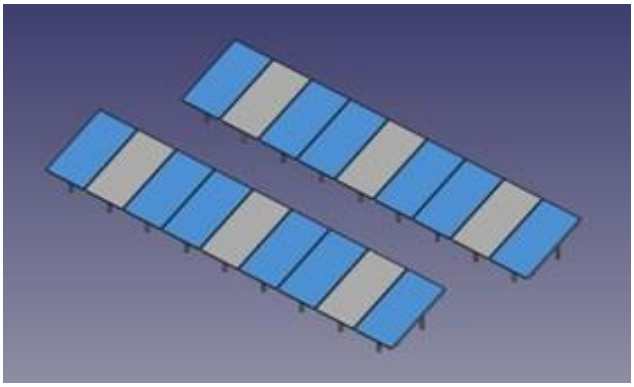

Figure 2. Two rows of arrays (9 by 2).

Before running simulations, the geometries created had to go through a process called meshing, which is the process of dividing a CAD model into multiple small cells (mathematically defined shapes) that can be used to discretize a domain in order to simplify a geometry's complexity and to whom the governing equations are applied when solving simulations.

The final step before proceeding to simulations was to setup the solver. It was where fluid material properties, boundaries and the flow physics model were defined. As a thermal analysis was not performed, the materials assigned to the rows of PV panels were neglected – the geometry was only defined as a solid. However, the fluid inside the wind tunnel must be air, obviously. Wind tunnel structure does not present any requirement in what concerns materials; in spite of that, it inevitably needed boundaries designation, which is a process based on imputing physical conditions to the boundaries of the flow domain – the so-called boundary conditions. They are inherent to the wind model applied to the wind tunnel, that is detailed right away. That being said, the boundary conditions set were: inlet – velocity type, with magnitudes of W_{max} and W_{avg} (steady-state); outlet – pressure type, equal to zero (steady-state); top and sides – slip/symmetry type. Once the front of the PV geometry is facing the inlet, wind flow is parallel to planes xOy and yOz and perpendicular to xOz.

Finally, with the understanding that wind is a fluid flow, when simulation the wind influence on photovoltaic panels, it was decided to neglect its laminar phase, since it is well known that the laminar phase of a flow (smooth path with no disruption between adjacent paths) is much smaller than its turbulent one (chaotic path that comprises eddies, swirls and flow instabilities) in the type of problem studied here. Thereby, a turbulent flow k-ε (which is the default turbulence model in Autodesk CFD) was applied as an external flow in the longitudinal direction of the wind tunnel, at the inlet. The standard model was chosen by virtue of its characteristics: it gives accurate predictions on distribution of speed around CAD geometries [29] and it is a general purpose model (the most used) that performs well for a large number of applications. The model is part of the Reynolds-Average Navier Stokes (RANS) family of turbulence models and both letters that name it refer to two transport equations that are solved upon its usage: turbulent kinetic energy – energy in turbulence – and turbulent dissipation rate – rate of dissipation of turbulent kinetic energy –, respectively.

3. Results

Wind flow around the PV arrays was analysed for each geometry, taking into consideration the two aforementioned wind velocities at the inlet: W_{avg} = 4.06 m/s and W_{max} = 17.55 m/s. In order to extract valuable information about

turbulent flow behaviour, a vertical plane – parallel to yOz and perpendicular to xOz – was applied to the wind tunnel, for each geometry and for each inlet wind speed. This generated a cross section inside the tunnel's volume, where it can be observed the wind flow pattern. With the purpose of obtaining a general wind flow distribution around the whole geometries, a rectangular grid of points was defined at the inlet. Each of these points generates a path across the tunnel for the corresponding wind element point, creating a continuous line.

In what the first CAD model is concerned (3 by 2 geometry), its simulations results for W_{avg} are shown in Figures 3 and 4. For the first one, the vertical plane is aligned with the central module of both rows, given that they are parallel (x and z coordinates are equal). For the later one, the plane is aligned with the tip module of each array. The left side scale indicates the velocity magnitude in cm/s, starting in 0 cm/s and ending in 514.366 cm/s for all the figures that refer to this wind speed value. It was observed that the wind shadow phenomenon introduced earlier occurs, which implies a decrease in wind speed right after the first array, thus leading to a lower wind intensity for the second row. When inspecting the wind behaviour close to the front PV module, it was possible to verify that wind has higher speed magnitudes in the upper portion of its face. Although this also happens to the equivalent panel of the second row, the magnitudes are much different, which will cause disparities between temperatures of the modules.

It can be said that despite the fact that turbulent flows are not likely to be perfectly predictable, there is approximately a symmetry of wind flow distribution thus wind speed distribution from the middle of each row to each of its extremities.

Consequently, there is no need to show wind flow simulations for both of them. By examination of the cross section that represents wind flow for the surroundings of the tip modules of each row, it was seen that the wind shadow effect is attenuated, hence the rear panel presents higher speed values near its face if compared to the central module. At the same time, it is clear that wind has a not so different behaviour for all the front row modules when compared to the rear set.

Figure 5, which is also a side view that allows the perception of wind movement along the wind tunnel when crossing the whole PV structure, made evident the appearance of swirls that differ from the common motion of the fluid, as they are represented mostly by blue lines after each array. These swirls are the so-called eddies in fluid mechanics. Their energy is successively transferred from large eddies to smaller ones until it is dissipated [30]. This figure confirms wind shadowing between rows of panels by two factors: reduction of lines density and mitigation of wind speed.

The same procedure was repeated for W_{max}, where similar results were obtained proportionally, i.e., the wind behaviour was verified as identical, but wind speeds presented higher magnitudes and turbulent events were enhanced.

Next, wind velocity values were collected for a very close vicinity of the panels' faces. These values are shown in Table 2, in which the parcel Ratio indicates the ratio between the wind speed collected and the inlet speed value. Note that the numbering of panels is done from left to right and it starts in the left tip panel of the first row.

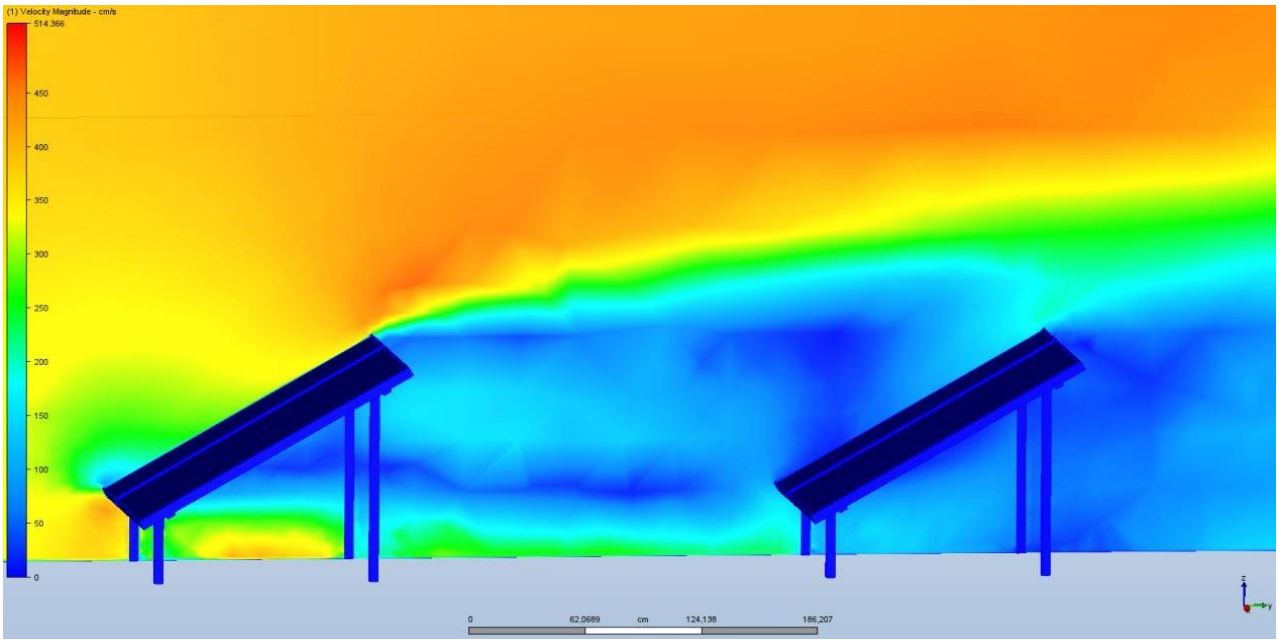

Figure 3. Wind flow for a vertical panel aligned with central module of the 3 by 2 geometry – W_{avg}.

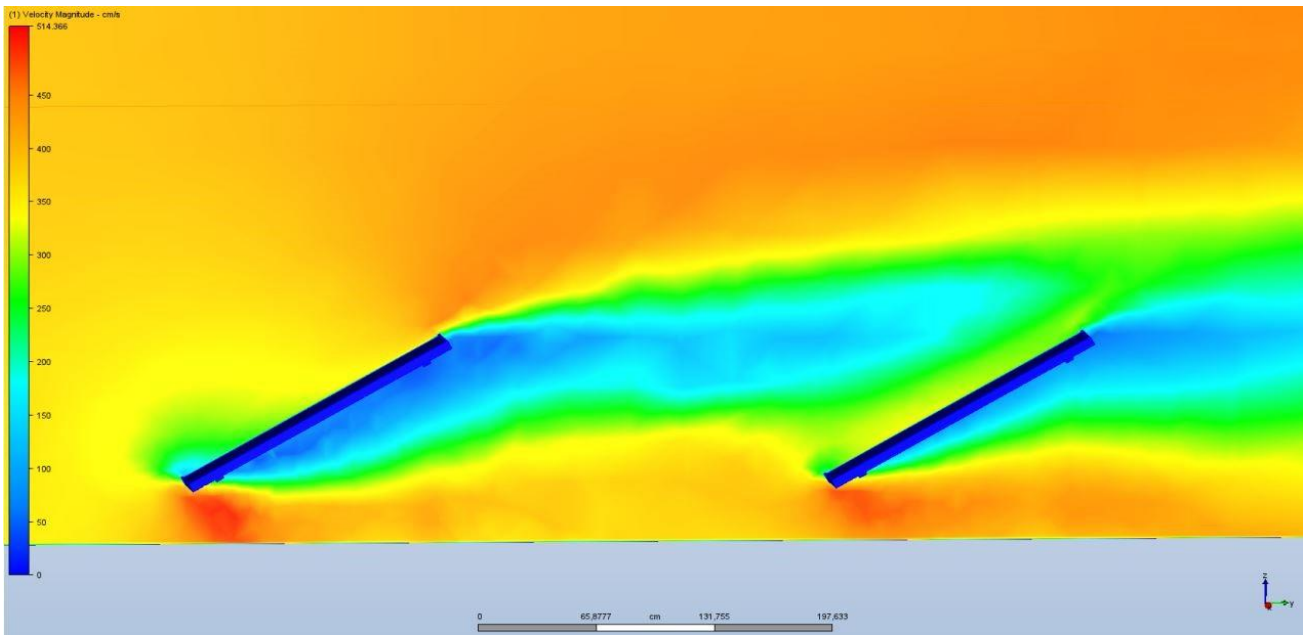

Figure 4. Wind flow for a vertical plane aligned with tip module of the 3 by 2 geometry – W_{avg}.

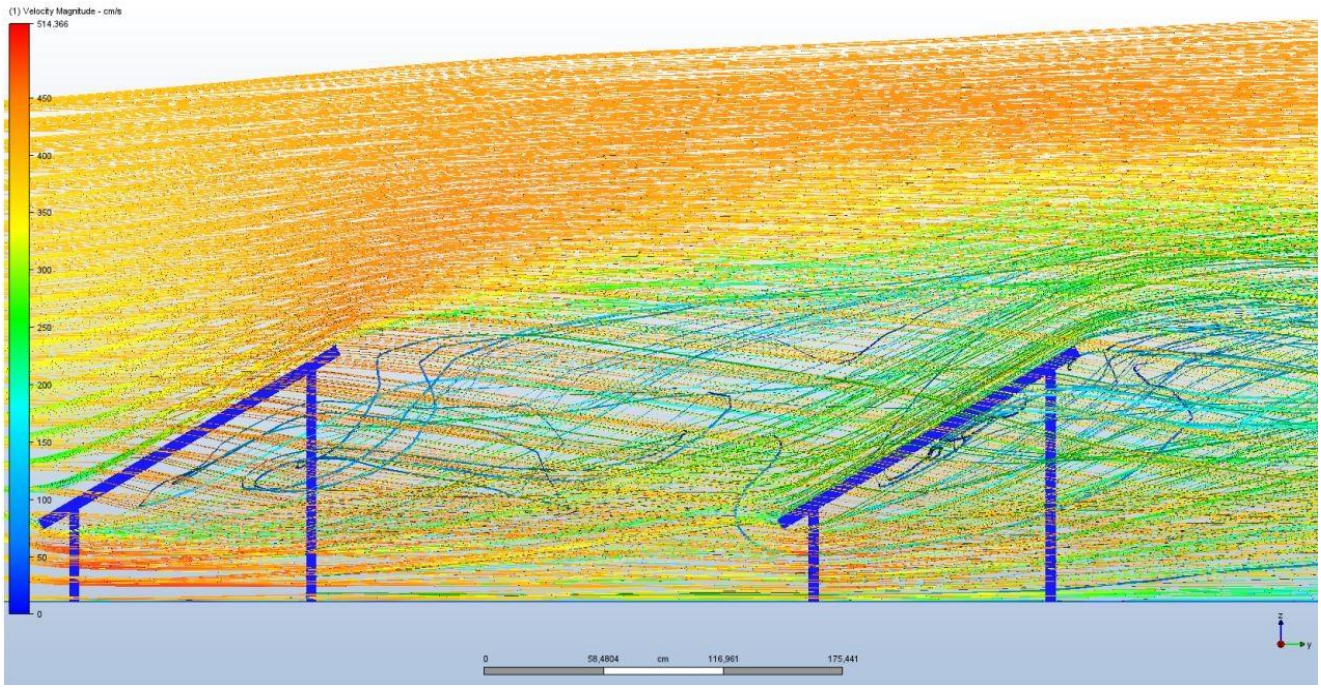

Figure 5. Side view of wind flow for the 3 by 2 geometry – W_{avg}.

Table 2. Wind speed for each panel (3 by 2 geometry).

	W_{avg} Speed (m/s)	Ratio	W_{max} Speed (m/s)	Ratio
Panel 1	2.7700	0.6823	12.3322	0.703
Panel 2	2.5737	0.6339	11.4047	0.650
Panel 3	2.7617	0.6802	12.2184	0.696
Panel 4	2.6932	0.6634	12.1172	0.690
Panel 5	1.3441	0.3311	5.9081	0.337
Panel 6	2.6806	0.6602	12-0584	0.687

By comparison of the values for both wind speed values, their similarity in what the ratio is concerned is truly evident. There is a significant decrease of wind speed for the central module of the second row (panel 5) but the effective difference between panel 1 and 4 and between 3 and 6 is almost unnoticeable; although the distribution of wind speed may not be so alike, the average wind speed values are.

The 3 by 2 geometry presents a reduced complexity when compared to the geometry covered in this subsection. Although it can represent a real-life situation in such a manner that the simulations results detailed before are a very

coherent starting point for what can be expected for other arrangements, the most common designs found in solar plants are clearly more similar to this second one. This being said, each of the tasks performed for the simpler CAD model were replicated to the 9 by 2 geometry.

Starting by the analysis of simulations related to W_{avg}, a vertical plane was applied to the wind tunnel, as it can be seen in Figure 6, generating a cross section along the PV structure and the tunnel. This figure depicts the wind flow for the area represented by the plane. The scale displayed in the left side of the figures that illustrate the average average wind speed at the inlet indicates the velocity magnitude, starting in 0 cm/s and goes up to 645.984 cm/s. As it was done for the previous geometry, the plane is aligned with the central module of the 9 by 2 geometry. Once again, the wind shadow effect can be observed due to the much lower wind speed verified for the surroundings of the rear module.

Figure 7 shows wind flow when the vertical plane is aligned with the tip modules. By its inspection, it was possible to confirm that just like with the preceding geometry, wind shadowing effect is almost null for the modules at the extremities.

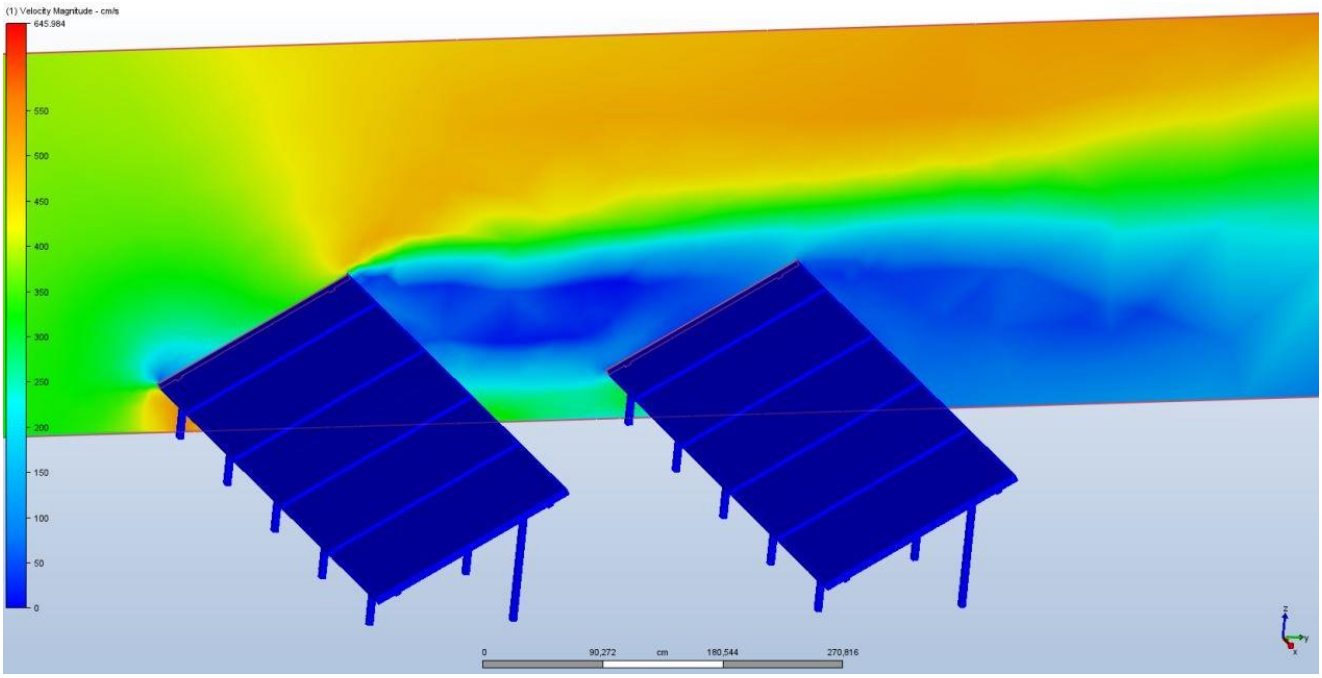

Figure 6. Wind flow for a vertical panel aligned with central module of the 9 by 2 geometry – W_{avg}.

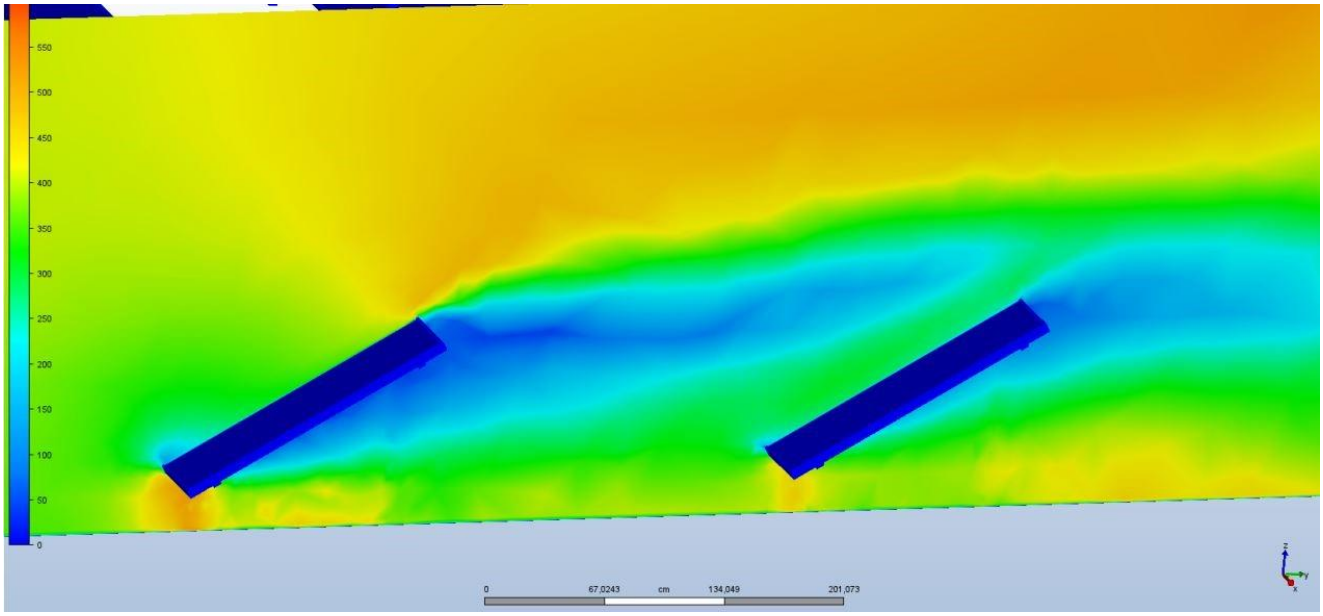

Figure 7. Wind flow for a vertical panel aligned with tip module of the 9 by 2 geometry – W_{avg}.

Wind velocity values were also collected for this geometry respecting to each of the velocities at the inlet, W_{avg} and W_{max}. These values are exhibited in Table 3. By its inspection, it was noticed an abrupt difference between the wind

speeds registered for the tip modules of the rear row (panels 18 and 10) and the remaining, as expected. There is a clear difference between both scenarios: for a lower velocity at the inlet, the ratios observed for the tip panels of each row (1 and 10, 9 and 18) decrease substantially from the front to the rear row, but for a higher wind velocity at the inlet, the wind shadow effect is reduced for the tip panels, which leads to a similar ratio when comparing wind speed for panel 1 with 10 and panel 9 with 18 for this velocity – relations that are closer to what was verified for the first geometry.

Table 3. Wind speed for each panel (9 by 2 geometry).

Panel	W_{avg} Speed (m/s)	Ratio	Panel	W_{avg} Speed (m/s)	Ratio
Panel 1	2.8307	0.6972	Panel 10	2.0932	0.5156
Panel 2	2.5662	0.6321	Panel 11	0.8621	0.2123
Panel 3	2.4935	0.6142	Panel 12	0.7557	0.1861
Panel 4	2.4389	0.6007	Panel 13	0.7445	0.1834
Panel 5	2.4498	0.6034	Panel 14	0.7180	0.1769
Panel 6	2.4767	0.6100	Panel 15	0.7561	0.1862
Panel 7	2.5241	0.6217	Panel 16	0.7959	0.1960
Panel 8	2.5407	0.6258	Panel 17	0.8583	0.2114
Panel 9	2.7356	0.6738	Panel 18	2.1541	0.5306
Panel	**W_{max} Speed (m/s)**	**Ratio**	**Panel**	**W_{max} Speed (m/s)**	**Ratio**
Panel 1	13.2141	0.7529	Panel 10	12.3679	0.7047
Panel 2	11.9650	0.6818	Panel 11	3.4115	0.1944
Panel 3	11.5708	0.6593	Panel 12	2.6822	0.1528
Panel 4	11.4064	0.6499	Panel 13	2.8797	0.1641
Panel 5	11.4009	0.6496	Panel 14	2.8360	0.1616
Panel 6	11.4496	0.6524	Panel 15	2.9946	0.1706
Panel 7	11.6691	0.6691	Panel 16	2.8800	0.1641
Panel 8	11.9045	0.6783	Panel 17	3.2980	0.1879
Panel 9	13.0969	0.7463	Panel 18	12.2337	0.6971

Temperature predictions were only performed for the second geometry (9 by 2), which depicts a more common case in solar plants. In addition to that, due to the similarities verified for wind flow for both of the geometries under study, it would be almost redundant to calculate the temperatures for each geometry. That being so, the calculations for the 9 by 2 geometry were done according to the following: module temperature forecast according to each prediction model; for each prediction model, each PV Having said that, Table 4 shows the values of temperature (in °C) predicted by each model, taking into account each PV technology and the two distinct wind speed values used in CFD simulations, W_{avg} = 4.06 m/s and W_{max} = 17.55 m/s. Each of the values displayed refers to a single average temperature value for each set of 18 panels. As it was aforesaid, it is important to mention that models Skoplaki 1, Skoplaki 2, Koehl, Mattei 1 and Mattei 2 take into consideration technology-relative parameters, whereas Kurtz and Tamizhmani do not. This is the reason why the temperatures are the same for the same values of wind speed, disregarding technologies.

Remembering that the Standard Approach is the reference model, which does not account with wind data (it just has an implicit wind velocity of 1m/s associated), the variation of the temperatures predicted by the models that take wind data into account compared with the standard model is very significant: the maximum absolute variation (worst case) between the results predicted by the complex models is 8.18 °C, but it is increased to 18.73 °C when compared with the SA – this type of discrepancy is much more common throughout all the comparisons between the other models with the Standard Approach than with one another. By inspection of Table 4, it is visible that the Skoplaki models predict lower temperatures than the other models for every technology; the Koehl model is the one that exhibits higher variations with the various technologies; the Mattei models present very similar temperatures across all the technologies and the results they generated are identical between both models, never showing a variation of more than 1.04 °C; the Kurtz and Tamizhmani models predicted close temperatures between them for W_{avg}, but differ for higher wind speeds. One interesting case that deviates from all the others is the prediction performed by the Koehl model for the CIGS technology at W_{avg}, which is slightly higher than the value expected by the NOCT formula.

It was noticed that the predicted temperatures are always lower for W_{max} in contrast to W_{avg}, which clarifies the influence that wind has as a cooling mechanism for solar photovoltaic modules. The higher the speed, the lower the temperature predicted according to the module temperature prediction models. These variations in temperature can make all the difference in the output power of the panels, since high temperatures reduce modules efficiency.

Taking into consideration the temperatures predicted in the previous section, the corresponding output power variations were calculated. Knowing that the SA is the reference model, it can be assumed that its predictions correspond

to the temperatures commonly expected and these temperatures correspond to a certain power output variation. Being that all the temperatures predicted by the different models are lower than the ones foreseen by the NOCT formula, except for the case mentioned above, the values displayed in Table 5 are the difference between the temperatures predicted by the models that take wind data into account and the values anticipated by the Standard Approach multiplied by the temperature coefficient of Pmpp. Given that β_{STC} units are %/°C, the results obtained are in percentage.

The interpretation of Table 5 is that wind speed (W_{avg} or W_{max}) has an influence such that its flow increases/decreases output power in x% when compared with the output power variation normally expected by the SA, in which wind is not taken into consideration.

Table 4. Values of temperature in °C for each set of 18 PV panels.

Technology	**poly-Si**		**CdTe**		**CIGS**	
Wind speed	W_{avg}	W_{max}	W_{avg}	W_{max}	W_{avg}	W_{max}
SA	45		45		47	
Skoplaki 1	36.81	27.44	36.56	27.33	38.69	28.27
Skoplaki 2	37.70	29.30	37.44	29.16	39.67	30.34
Koehl	39.63	31.01	44.53	33.36	47.38	35.90
Mattei 1	39.64	33.73	39.22	33.44	40.02	34.01
Mattei 2	40.67	33.34	40.22	33.06	41.06	33.61
Kurtz	42.30	35.51	42.30	35.50	42.30	35.51
Tamizhmani	42.78	32.55	42.78	32.55	42.78	32.55

Table 5. Output power variation in percentage (%) for each set of 18 PV panels.

Technology	**poly-Si**		**CdTe**		**CIGS**	
Wind Speed	W_{avg}	W_{max}	W_{avg}	W_{max}	W_{avg}	W_{max}
Skoplaki 1	3.19	6.85	2.36	4.95	2.58	5.81
Skoplaki 2	2.85	6.12	2.12	4.43	2.27	5.16
Koehl	2.09	5.45	0.13	3.26	−1.20	3.44
Mattei 1	2.09	4.40	1.62	3.24	2.16	4.03
Mattei 2	1.69	4.55	1.34	3.34	1.84	4.15
Kurtz	1.05	3.70	0.76	2.66	1.46	3.56
Tamizhmani	0.87	4.86	0.62	3.49	1.31	4.48

4. Conclusions

This paper was developed with the main purpose of studying the influence of wind in energy generation of solar plants. To accomplish this task, several parameters were analysed, which culminated in the decision of giving preference to the investigation of how wind could perform as a natural cooling mechanism for solar photovoltaic modules in solar plants look-alike arrangements of PV arrays. Delving into the several methods one could use to examine the interaction between wind flow and modules temperature, it was decided to follow empirical models that predict panels temperature according to various wind speeds and technology-based parameters (for most of them). Given that individual technologies present intrinsic properties, the temperatures that would be foreseen would tend to vary from technology to technology. The understanding of this fact led to the choice of three technologies in vogue worldwide (by distinct factors). Due to the fact that it would not be plausible to compare wind flow around geometries of different sizes, it was assumed that all three had exactly the same proportions, but with different parameters that would characterise each of them; since the variables used in the temperature prediction models are technology-related, dimensions could be neglected.

That being said, a Computational Fluid Dynamics analysis of the wind flow around PV geometries was done with the intention of collecting data on wind speeds close to the solar photovoltaic panels. It was observed that for the direction of wind studied, the front rows of photovoltaic arrays always show higher wind velocity magnitudes, which are similar to the ones registered for the tip panels of the rear rows; the occurrence of wind shadowing between rows of panels imply lower wind speeds for most back panels. The referred data were used in the calculations related to the modules temperature predictions that were subsequently crucial to the output power variation results calculated for each scenario. To execute this assignment, it was imperative to use factual wind information that was gathered from reliable sources, thus empowering simulations of concrete circumstances, mimetizing a real-life approach.

The results achieved expose that higher wind speeds are directly related to decreases in modules temperature: for the average wind speeds verified for Lisbon in 2020, variations of output power reached 3.19 percentage points, which expresses a very significant amount of electrical energy production when talking about solar plants. For the highest

wind velocities, a maximum variation of 6.85 percentage points in power output was registered. Despite the fact that these last are not the most common values for wind velocities, they are always recorded at some moment, hence their relevance in this research.

One decisive factor that has to be taken into account is that the results attained are highly dependent on the values of wind speeds collected through simulations, on the parameters found in solar panels datasheets and, finally, on the accuracy of the temperature prediction modules employed. To what the wind speeds collected are concerned, the abrupt differences in velocity around the panels influence the calculations made in a critical way. In order to interpret the calculations results displayed in this paper correctly, it must be foreknown that the wind speed value collected for each solar photovoltaic panel involves an area right after the surface of the PV panels, where wind speeds have lower magnitudes. This procedure leads to lower temperatures variation and lower output power variations. With this in mind, it can be said that the results here achieved allude to the worst case (although its just-proven benefits), from an electrical engineering perspective.

Taking into consideration the results obtained, it can be said that, in fact, wind works as a natural cooling mechanism for solar panels, thereby improving their productivity, which can lead to significant benefits respecting electrical energy production in solar plants. Nevertheless, several other factors that are correlated with wind loads must be investigated and should not be neglected when thinking about wind's influence on solar plants.

To the extent of the reliances explained for the final results herein presented, this work cannot be considered a dogma for projects with the same technologies here studied or for every scenario, but it is manifested as a general approach that certainly contributes to a strong insight on how wind influences the electrical energy production in solar plants through its cooling effects.

Acknowledgments

This work was supported in part by FCT/MCTES through national funds and in part by cofounded EU funds under Project UIDB/50008/2020. Also, this work was supported by FCT under the research grant UI/BD/151091/2021.

Author Contributions

C.B.: Conceptualization, software, methodology, formal analysis; R.A.M.L.: Conceptualization, Writing – Review & Editing; C.P.C.V.B.: Conceptualization, Writing – Review & Editing; J.P.N.T.: Conceptualization, software, methodology, investigation, formal analysis, supervision. All authors have read and agreed to the published version of the manuscript.

Ethics Statement

Not applicable.

Informed Consent Statement

Not applicable.

Funding

This research received no external funding.

Declaration of Competing Interest

The authors declare that they have no known competing financial interests or personal relationships that could have appeared to influence the work reported in this paper.

References

1. Torres JPN, Marques Lameirinhas RA, Correia Valério Bernardo CP, Lima Martins S, Mendonça dos Santos P, Veiga HI, et al. Analysis of Different Third-Generation Solar Cells Using the Discrete Electrical Model d1MxP. *Energies* **2023**, *16*, 3289.
2. Marques Lameirinhas RA, Correia V. Bernardo CP, Torres JPN, Veiga HI, Mendonça dos Santos P. Modelling the effect of defects and cracks in solar cells' performance using the d1MxP discrete model. *Sci. Rep.* **2023**, *13*, 12490.
3. European Comission. 2020 Climate & Energy Package. Available online: https://ec.europa.eu/clima/policies/strategies/2020 (accessed on 14 May 2020).
4. Marques Lameirinhas RA, Torres JPN, de Melo Cunha JP. A Photovoltaic Technology Review: History, Fundamentals and Applications. *Energies* **2022**, *15*, 1823.

5. Alves dos Santos SA, Torres JPN, Ferreira Fernandes CA, Marques Lameirinhas RA. The impact of aging of solar cells on the performance of photovoltaic panels. *Energy Convers. Manag. X* **2021**, *10*, 100082.
6. Associacao Portuguesa de Energias Renovaveis. Balanco da producao de eletricidade de portugal continental (abril de 2020). Available online: https://www.apren.pt/pt/energias-renovaveis/producao (accessed on 16 May 2020).
7. Santos MS, Marques Lameirinhas RA, Torres JPN, Fernandes JFP, Correia V. Bernardo CP. Nanostructures for Solar Energy Harvesting. *Micromachines* **2023**, *14*, 364.
8. Stefani BV, Kim M, Zhang Y, Hallam B, Green MA, Bonilla RS, et al. Historical market projections and the future of silicon solar cells. *Joule* **2023**, *7*, 2684–2699.
9. International Energy Agency. Renewables, 2019. Available online: https://www.iea.org/reports/renewables-2019 (accessed on 14 May 2020).
10. Smets AHM, Jager K, Isabella O, van Swaaij R, Zeman M. *Solar Cell Parameters and Equivalent Circuit*; UIT Cambridge Limited: Cambridge, UK, 2016.
11. Tamizhmani G, Ji L, Tang Y, Petacci L, Osterwald C. Photovoltaic module thermal/wind performance: Longterm monitoring and model development for energy rating. In Proceedings of the NCPV and Solar Program Review Meeting, Denver, CO, USA, 24–26 March 2003; pp. 936–939.
12. Ruscheweyh H, Windhovel R. Wind loads at solar and photovoltaic modules for large plants. In Proceedings of the 13th International Conference on Wind Engineering, Amsterdam, The Netherlands, 10–15 July 2011.
13. Schwingshackl C, Petitta M, Wagner JE, Belluardo G, Moser D, Castelli M, et al. Wind effect on PV module temperature: Analysis of different techniques for an accurate estimation. *Energy Procedia* **2013**, *40*, 77–86.
14. Florschuetz LW. Extension of the Hottel-Whillier model to the analysis of combined photovoltaic/thermal flat plate collectors. *Solar Energy* **1979**, *22*, 361–366.
15. Markvart T. *Solar Electricity*, 2nd ed.; John Wiley & Sons Ltd.: Chichester, UK, 2000.
16. Skoplaki E, Palyvos JA. Operating temperature of photovoltaic modules: A survey of pertinent correlations. *Renew. Energy* **2009**, *34*, 23–29.
17. Duffie JA, Beckman WA. *Solar Engineering of Thermal Processes*, 4th ed.; Wiley: Hoboken, NJ, USA, 2013.
18. Armstrong S, Hurley WG. A thermal model for photovoltaic panels under varying atmospheric conditions. *Appl. Therm. Eng.* **2010**, *30*, 1488–1495.
19. Koehl M, Heck M, Wiesmeier S, Wirth J. Modeling of the nominal operating cell temperature based on outdoor weathering. *Solar Energy Mater. Solar Cells* **2011**, *95*, 1638–1646.
20. Faiman D. Assessing the Outdoor Operating Temperature of Photovoltaic Modules. *Wiley InterScience* **2008**, *16*, 307–315.
21. Mattei M, Notton G, Cristofari C, Muselli M, Poggi P. Calculation of the polycrystalline PV module temperature using a simple method of energy balance. *Renew. Energy* **2006**, *31*, 553–567.
22. Kurtz S, Miller D, Kempe M, Bosco N, Whitefield K, Wohlgemuth MJ, et al. Evaluation of High-Temperature Exposure of Photovoltaic Modules; Preprint; NREL: Golden, CO, USA, 2009; pp. 2399–2404.
23. Amajama J, Ogbulezie JC, Akonjom NA, Onuabuchi VC. Impact of wind on the output of photo-voltaic panel and solar illuminance/intensity. *Int. J. Eng. Res. Gen. Sci.* **2016**, *4*, 137–142.
24. Hu HH. Chapter 10 - Computational Fluid Dynamics. In *Fluid Mechanics*, 5th ed.; Academic Press: Boston, MA, USA, 2012; pp. 421–472.
25. BYD. 156.57p - series - 4bb. Available online: https://sg.byd.com/wpcontent/uploads/2017/10/combine-4-1 (accessed on 23 April 2021).
26. First Solar. First Solar Series 4 pv module. Available online: https://www.firstsolar.com/enEmea/-/media/First-Solar/Technical-Documents/Series-4 (accessed on May 2023).
27. Available online: https://www.firstsolar.com/en-Emea/-/media/First-Solar/Technical-Documents/Series-4-Datasheets/Series-4V3-Module-Datasheet.ashx (accessed on 23 April 2021).
28. Solar Frontier. Product Data Sheet sf170-s. Available online: https://www.solarfrontier.com/eng/solutions/products/pdf/datesheat170.pdf (accessed on 23 April 2021).
29. Autodesk. Wind Tunnel. Available online: https://knowledge.autodesk.com/searchresult/caas/CloudHelp/cloudhelp/ENU/FlowDesign/files/GUID (accessed on May 2023).